Electronic Supplementary Material (ESI) for Journal of Materials Chemistry C.
This journal is © The Royal Society of Chemistry 2021

Less is More: On the Effect of Benzannulation on Solid-State Emission of Difluoroborates

Iryna Knysh,[†] Anna Kozakiewicz-Piekarz,[‡] Andrzej Wojtczak,[‡] Damian Plażuk,[¶] Glib Baryshnikov,[§,‖] Rashid Valiev,[⊥,#] Rinat Nasibullin,[⊥] Hans Ågren,[@] Denis Jacquemin[⋆,△] Borys Ośmiałowski[⋆,‡] and Robert Zaleśny[⋆,†]

†*Faculty of Chemistry, Wrocław University of Science and Technology, Wyb. Wyspiańskiego 27, PL–50370 Wrocław, Poland*

‡*Faculty of Chemistry, Nicolaus Copernicus Univ., Gagarina 7, PL-87100 Toruń, Poland*

¶*Laboratory of Molecular Spectroscopy, Department of Organic Chemistry, Faculty of Chemistry, University of Łódź, Tamka 12, PL-91-403 ,Łódź Poland*

§*Linköping University, Department of Science and Technology, Laboratory of Organic Electronics, Norrköping, SE-60174 Sweden*

‖*Department of Chemistry and Nanomaterials Science, Bohdan Khmelnytsky National University, Cherkasy, Ukraine*

⊥*Tomsk State University, Tomsk 634050, Russia*

#*Department of Chemistry, University of Helsinki, Helsinki FIN – 00014, Finland*

@*Department of Physics and Astronomy, Uppsala University, Box 516, SE-751 20 Uppsala, Sweden*

△*Université de Nantes, CNRS, CEISAM UMR 6230, F-44000 Nantes, France*

E-mail: Denis.Jacquemin@univ-nantes.fr; Borys.Osmialowski@umk.pl; Robert.Zalesny@pwr.edu.pl

Table of content

Experimental one-photon absorption and emission data

Table S1: Spectroscopic features of **1-4** in different solvents[a] and in the solid state: absorption (λ_{abs}; nm), fluorescence maxima (λ_{fl}; nm), fluorescence quantum yield (Φ_{f}), radiative (k_{r}; 10^8 s^{-1}) and non-radiative (k_{nr}; 10^8 s^{-1}) rate constants.

	MCH[b]	**Et$_2$O**[c]	**CHCl$_3$**[d]	**THF**[e]	**EA**[f]	**AcMe**[g]	**MeOH**[h]	**MeCN**[i]	**DMF**[j]	**SS**[k]
1										
λ_{abs}	413 433.5	413	426	420	416	417	418	417	423	–
λ_{fl}	447 471	477	490	499	499	514	517	528	530	563
Φ_{f}	0.519	0.868	0.705	0.684	0.699	0.569	0.454	0.517	0.382	0.314
k_{r}	3.18	3.60	3.01	2.68	2.71	2.25	2.26	2.00	1.57	–
k_{nr}	2.95	0.55	1.26	1.24	1.17	1.70	2.72	1.87	2.53	–
2										
λ_{abs}	473	467	477	472	468	468	468	468	474	–
λ_{fl}	478 510	509	521	540	534	562	564	573	581	645
Φ_{f}	0.862	0.747	0.860	0.517	0.614	0.374	0.308	0.296	0.187	< 0.01
k_{r}	3.79	2.92	3.07	1.83	2.26	1.58	2.01	1.56	1.23	–
k_{nr}	0.61	0.99	0.50	1.71	1.42	2.65	4.51	3.71	5.34	–
3										
λ_{abs}	462	458	466	462	458	460	458	458	464	–
λ_{fl}	478 504	503	512	528	520	541	540	552	555	600
Φ_{f}	0.979	0.848	0.743	0.658	0.663	0.587	0.499	0.638	0.561	0.020
k_{r}	4.63	3.57	3.17	2.51	2.48	2.06	1.82	2.20	1.90	–
k_{nr}	0.10	0.64	1.10	1.31	1.26	1.45	1.83	1.25	1.49	–
4										
λ_{abs}	474	472	483	478	475	477	475	476	484	–
λ_{fl}	485	513	521	539	536	559	559	569	571	611
Φ_{f}	1.000	0.999	0.811	0.585	0.655	0.441	0.471	0.447	0.323	0.063
k_{r}	4.65	3.93	3.12	2.06	2.42	1.53	2.12	1.68	1.38	–
k_{nr}	0.00	0.003	0.73	1.47	1.27	1.94	2.38	2.08	2.88	–

[a] Solvents in the Table are ordered according to increasing magnitude of their dipole moment. [b] Methylcyclohexane. [c] Diethyl ether. [d] Choloroform. [e] Tetrahydrofuran. [f] Ethyl acetate. [g] Acetone. [h] Methanol. [i] Acetonitrile. [j] Dimethylformamide. [k] Solid state.

Calculations of photophysical properties

The theoretical fluorescence quantum yield ($\Phi_\mathrm{f}^\mathrm{theory}$) was calculated as follows

$$\Phi_\mathrm{f}^\mathrm{theory} = \frac{k_\mathrm{r}}{k_r + k_\mathrm{nr}} = \frac{k_\mathrm{r}}{k_\mathrm{r} + k_\mathrm{ic} + k_\mathrm{isc}} \tag{1}$$

where k_r is radiative rate constant, k_nr - non-radiative rate constant, k_ic - internal conversion rate constant, k_isc - intersystem crossing rate constant. All calculations were done in the gas phase.

Table S2: Excited states properties and spin–orbit coupling matrix elements (SOCME) for **1**-**4** calculated at the XMC-QDPT2(10,10)/6-31G(d,p) level of theory.

Compound	S_1, eV (f^a)	T_1, eV	T_2, eV	SOCME, cm^{-1}
1	2.80 (0.29)	2.64	3.02	0.36
2	2.81 (0.40)	2.75	2.90	0.19
3	3.00 (0.45)	2.70	3.30	0.30
4	2.49 (0.74)	2.23	2.96	1.00

[a] f is oscillator strength.

Table S3: Photophysical rate constants and non-adiabatic coupling matrix elements (NACME) calculated at the XMC-QDPT2(10,10)/6-31G(d,p) level of theory for **1**-**4**.

Compound	Photophysical parameters				
	$k_\mathrm{r}(S_1 \rightarrow S_0)$, s^{-1}	$k_\mathrm{ic}(S_1 \rightarrow S_0)$, s^{-1}	$k_\mathrm{isc}(S_1 \rightarrow T_1)$, s^{-1}	NACME, cm^{-1}	$\Phi_\mathrm{f}^\mathrm{theory}$
1	$9.8 \cdot 10^7$	$7.0 \cdot 10^5$	$5 \cdot 10^7$	0.02	0.66
2	$1.1 \cdot 10^8$	$4.7 \cdot 10^6$	$9 \cdot 10^7$	0.05	0.54
3	$1.7 \cdot 10^8$	$1.0 \cdot 10^6$	$8 \cdot 10^6$	0.02	0.95
4	$1.6 \cdot 10^8$	$1.0 \cdot 10^7$	$2 \cdot 10^8$	0.08	0.43

Table S4: Excited states properties and spin–orbit coupling matrix elements (SOCME) for **1**-**4** calculated at the TD-DFT/B3LYP/6-31G(d,p) level of theory.

Compound	S_1, eV (f^a)	T_1, eV	T_2, eV	SOCME, cm^{-1}
1	2.54 (0.15)	2.05	2.62	0.46
2	2.50 (0.40)	1.94	2.62	0.60
3	2.66 (0.55)	1.96	2.70	0.59
4	2.60 (0.60)	1.92	2.68	0.37

[a] The f is oscillator strength.

Table S5: Photophysical rate constants and non-adiabatic coupling matrix elements (NACME) calculated at the TD-DFT/B3LYP/6-31G(d,p) level of theory for **1**-**4**.

Compound	Photophysical parameters				
	$k_r(S_1 \rightarrow S_0)$, s^{-1}	$k_{ic}(S_1 \rightarrow S_0)$, s^{-1}	$k_{isc}(S_1 \rightarrow T_1)$, s^{-1}	NACME, cm^{-1}	Φ_f^{theory}
1	$4.1 \cdot 10^7$	$1.7 \cdot 10^6$	$2.0 \cdot 10^6$	0.03	0.92
2	$1.1 \cdot 10^8$	$4.7 \cdot 10^6$	$1.0 \cdot 10^6$	0.05	0.95
3	$1.7 \cdot 10^8$	$1.4 \cdot 10^6$	$1.3 \cdot 10^5$	0.03	0.99
4	$1.8 \cdot 10^8$	$2.0 \cdot 10^6$	$7.3 \cdot 10^4$	0.03	0.99

X-ray analysis

The X-ray structure of **2** is presented in Figure S1. The crystal X-ray experimental data can be found in Table S6. **2** is flat, the RMSD value calculated for atoms defining the ring system and two methyl groups of the NMe_2 moiety is 0.002 Å. Among these atoms, the significant displacement from the best plane is observed for B1 (0.111(2) Å) only. As a consequence, the non-identical displacement of fluorine atoms from that best plane is measured to be −0.962(1) and 1.307(1) Å for F1 and F2, respectively. This affects the dihedral angle between the difluoroborate-quinoline moiety and the C12–C17 phenyl ring, which is 1.19(8)° only. The displacement of B1 from the best plane of the B ring system leads to torsion angles of 2.6(2)° and −3.9(2)° for C10–C9–N1–B1 and C11–O1–B1–N1, respectively.

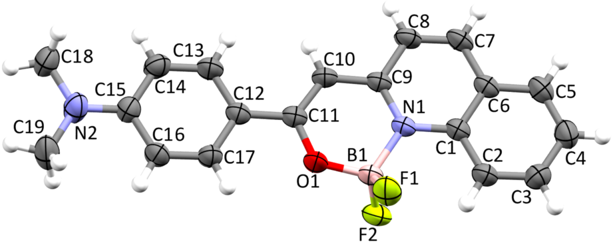

Figure S1: X-Ray crystal structure of **2**. The ellipsoid contour of probability level is 50%.

In the difluoroborate ring B, both C11–O1 (1.332(2) Å) and N1–C9 (1.357(2) Å) exhibit double bond character (Table S7). The C10–C11 bond, which is 1.362(2) Å long, is significantly shorter than expected for the single bond. This supports the presence of a significant electron delocalization between the N,N-dimethylaniline and quinoline moieties. The N1–B1 and B1–O1 bond lengths are 1.598(2) and 1.457(3) Å. The displacement of N1 from the B1–C9–C1 plane is 0.008 Å only. In the phenyl ring, both C13–C14 and C16–C17 possess double bond character, with respective lengths of 1.374(3) and 1.375(3) Å, values that are shorter by up to 10σ from other ring bonds [ranging from 1.397(2) (C12–C17) to 1.409(3) Å (C15–C16)]. The NMe_2 moiety is almost coplanar with the phenyl ring A, the dihedral angle between the best planes being as small as 1.68°. The deviation of N2 from the C15–C18–C19 plane is 0.023°.

The X-ray structure of **4** is presented in Figure S2. The crystal and X-ray experimental details can be found in Table S6. The whole difluoroborate-phenanthridine ring system is flat, with the RMSD value for atoms from the best plane being 0.003 Å. As in compound **2**, the difluoroborate ring B is planar with the RMSD value of atoms from the ring best plane of 0.003 Å. The B1 deviation is −0.003(4) Å only. The torsion angles C14–C13–N1–B1 and C15–O1–B1–N1 are 4.4(4) and −1.8(4)°, respectively. The F1 and F2 atoms are symmetrical positioned on opposite sides of the ring planes with displacement values of −1.143(1) (F1) and 1.124(2) Å (F2). Analysis of atomic displacement parameters (ADPs) in the difluoroborate ring reveals the significant oscillation amplitudes of the O–BF_2–N fragment in the direction perpendicular to the ring plane, hinting that a more dynamical behaviour of that fragment compared to the phenantridine ring system.

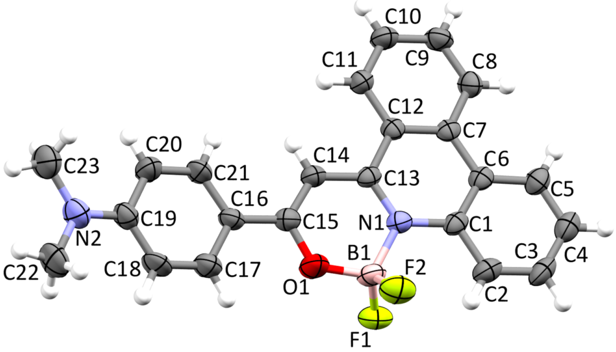

Figure S2: X-Ray crystal structure of **4**. The ellipsoid contour of probability level is 50%.

Similarly to compound **2**, in the difluoroborate ring moiety, the C15–O1 and C13–N1 bonds possess double bonds character, with respective distances of 1.320(3) and 1.347(3) Å, which are shorter than the corresponding distances in compound **2** (Table S7). The C14–C15 bond distance of 1.358(4) Å suggests the possible coupling of that fragment with the phenanthridine system. However, in contrast to **2**, a significant bend of the molecule is found with a 13.4(11)° dihedral angle between the phenanthridine ring system (B-C-D-E) and the phenyl ring A (Table S7). The rotation of the phenyl ring around C15–C16 leads to the torsion angle C14–C15–C16–C21 reaching −3.7(5)°. This indicates a slightly weakened coupling between the difluoroborate-phenanthridine system and 4-dimethylaminophenyl moiety. As in **2**, the C17–C18 and C20–C21 bond lengths in the phenyl ring, 1.369(4) Å, are significantly shorter than the other ring bonds ranging from 1.394(4) (C16–C21) to 1.405(4) Å (C19–C20). In the 4-dimethylaminophenyl moiety, the dihedral angle between the NMe_2 and the phenyl ring moieties is 4.5°, larger than in **2**. On the other hand, the displacement of N2 from the plane C19–C22–C23 is as small as 0.038 Å, suggesting an efficient electronic coupling between the dimethylamino group and the phenyl ring.

The X-ray structure of **3**, consisting of 3 molecules - **a**, **b**, **c**, is presented in Figure S3. The crystal and X-ray experimental details can be found in Table S6. Atoms in molecules **c**, **b**, and **a** are labelled as O1 – C19, O21 – C39 and O41 – C59, respectively. There are additional non-crystallographic relations between these molecules: molecules **c** and **b** are connected by a rotation around $[-0.057\ -0.090\ 1.000]$ by 175.97°; molecules **b** and **a** are related by a rota-inversion $[-1.000\ 0.189\ 0.001]$ by 174.59°; and there is a rota-inversion around [0.002 1.000 0.010] by −175.70° between molecules **c** and **a**.

The bond lengths in the phenyl rings of all molecules are close to the values expected for aromatic rings. However, the C13–C14 and C16–C17 bonds and their counterparts (for **b** and **a**) are slightly shorter than the other bonds, which is in agreement with the data obtained for both **2** and **4**. In **3** the differences between these two sets of bonds are the smallest within the series, indicating weaker coupling between the N,N-dimethylaniline moiety and the difluoroborate-isoquinoline system and smaller electronic delocalization.[1]

The distribution of double bonds in the difluoroborate ring is similar to that found in compounds **2** and **4**. However, some differences are observed between the molecules of **3** (Table S7). In molecule **c** the O1–B1 distance of 1.456(6) is slightly longer than the corresponding distances 1.435(6) and 1.438(6) in **b** and **a**, respectively. The B1–N1 and corresponding bonds in **b** and **a** are similar. The C11–O1 and its counterparts (O31–C21 and O41–C51) are in the 1.326(5) – 1.339(5) Å range, suggesting the double character of these bonds. The C9–N1 double bond (1.360(5) Å) in molecule **c** is significantly longer than

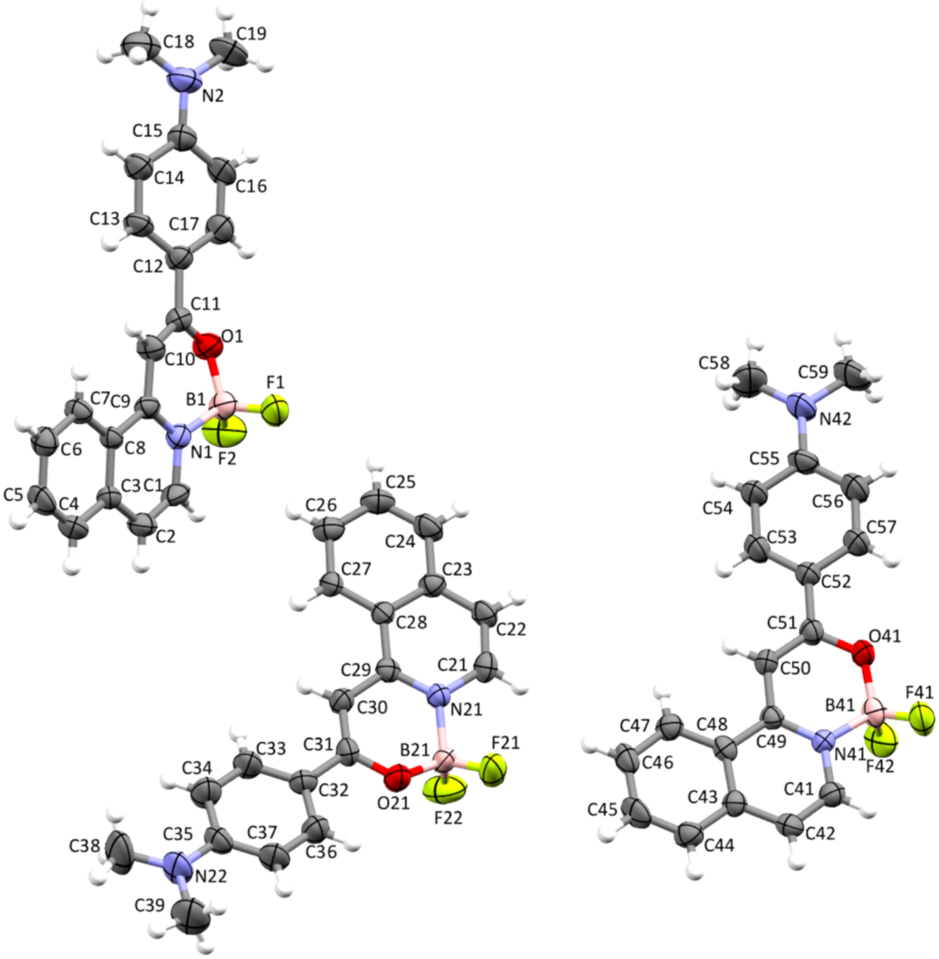

Figure S3: X-Ray crystal structure of **3**. Ellipsoids are contoured at 50% probability level.

the corresponding bonds in **b** (1.343(5) Å) and **a** (1.347(5) Å). Similar to **2** and **4**, the C10–C11 bond and its equivalents for **b** and **a** act as linkers between the ring systems enabling the delocalization over the whole molecules.

The difluoroborate ring of **3** is not flat. In three all molecules the largest atom displacements from the best plane are found for O1 and B1, and their equivalents. In molecule **c** the displacements are −0.132(4) (for O1) and −0.166(6) Å (for B1), and the largest torsion angles are C10–C9–N1–B1 −24.9(6)° and C9–N1–B1–O1 28.6(6)°. In molecule **b** the corresponding values for O21 and B21 displacements are −0.111(4) and 0.151(6) Å yielding torsion angles −24.0(6) to 25.7(7)°, while in molecule **a** these data attain −0.097(4) and 0.119(6) Å, and 18.9(7), −21.9(7)°, respectively. The displacements of the B atoms from the best planes of the difluoroborate rings are the largest amongst the compounds reported here. Therefore the potential coupling between difluoroborate ring and the isoquinoline (aromatic) moiety **3** is somehow weaker than in **2** and **4**.

All molecules are not flat. The dimethylamine group shows a slight rotation relative to the phenyl ring, with dihedral angle between the best planes of 2.3 (**c**) 1.96 (**b**), and 1.28° (**a**). In molecule **c**, the displacement of the N2 atom from the C15–C18–C19 plane is 0.046 Å. The corresponding distances are similar in molecules **b** (0.036 Å) and **a** (0.045 Å), and are the largest among studied structures. The dihedral angles between the phenyl and the isoquinoline rings are 15.5, 17.98, and 15.22° in molecules **c**, **b**, and **a**, respectively (Table S7). In molecules **c**, the dihedral angles between the B and C, C and E, and B and A rings (see labeling in Scheme 1) are 7.3(2), 0.3(2), and 14.8(2)°, respectively. The corresponding angles are 7.5(2), 0.6(2), and 14.8(2)° in molecules **b** and 3.8(2)°, 0.7(2)°, and 16.5(2)° in molecules **a**.

Crystal packing analysis

The labeling of the rings used in the current section can be found in Scheme 1.

The molecular packing of **2** is formed in slipped parallel motif (Figure S4a). The analysis of the packing reveals several types of intermolecular interactions including $\pi\cdots\pi$, C–H$\cdots\pi$, C–H$\cdots$O, and C–H$\cdots$F interactions (see Tables S7 and S8, Figure S4b). The $\pi\cdots\pi$ interactions are found between C and A$[1-X, 1-Y, 1-Z]$ rings with the Cg$\cdots$Cg (centroids) distance, dihedral angle between rings, angle between Cg and normal to the second ring, as well as slippage (distance between Cg1 and perpendicular projection of Cg2 on Ring 1) of 3.822(1) Å, 0.39(9)°, 19.0°, and 1.244 Å, respectively. The C$\cdots$A$[2-X, 1-Y, 1-Z]$ interaction is also found, the respective parameters being 3.764(1) Å, 2.08(9)°, 18.1°, and 1.172 Å, respectively. The B$\cdots$B$[2-X, 1-Y, 1-Z]$ interaction involving the difluoroborate rings is also observed with the above mentioned parameters of 3.912(1) Å, 0.02(8)°, 26.9°, and 1.772 Å. The aniline moiety ring A is involved in the A$\cdots$(B+C)$[\,1-X, 1-Y, 1-Z]$ and A$\cdots$(C+D)$[2-X, 1-Y, 1-Z]$ with key parameters 3.831(1) Å, 1.19(8)°, 20.3°, and 1.327 Å, and 3.712(1) Å, 2.53(8)°, 13.7°, and 0.881 Å, respectively. A C18–H18B$\cdots\pi$ interaction is found involving the C3–C8 fragment of the quinolone moiety D$[1-X, 1-Y, 1-Z]$, the H$\cdots$Cg distance being 2.98 Å and C-H$\cdots$Cg angle of 126°.

The asymmetric unit of **3** consists of 3 molecules - **a** (red), **b** (blue), and **c** (green) arranged in a "herring-bone" fashion (Figure S5a). The molecular packing reveals several intermolecular interactions types: $\pi\cdots\pi$, C–H$\cdots\pi$, C–H$\cdots$O, and C–H$\cdots$F interactions (Tables S7 and S8, Figure S5b). The extensive network of $\pi\cdots\pi$ interactions involves the symmetry related molecules of the same type. As a consequence the packing consists of layers of molecules built up exclusively of molecules **a**, **b**, or **c**. These interactions involve the six-membered rings including the difluoroborate moieties, or might be described with the stacking of the whole difluorobotate-isoquinoline systems.

Molecules **c** are involved in a series of $\pi\cdots\pi$ interactions. The difluoroborate ring B interacts with the rings of the neighbouring molecule **c** – B$[\frac{3}{2}-X, -\frac{1}{2}+Y, Z]$ and B$[\frac{3}{2}-$

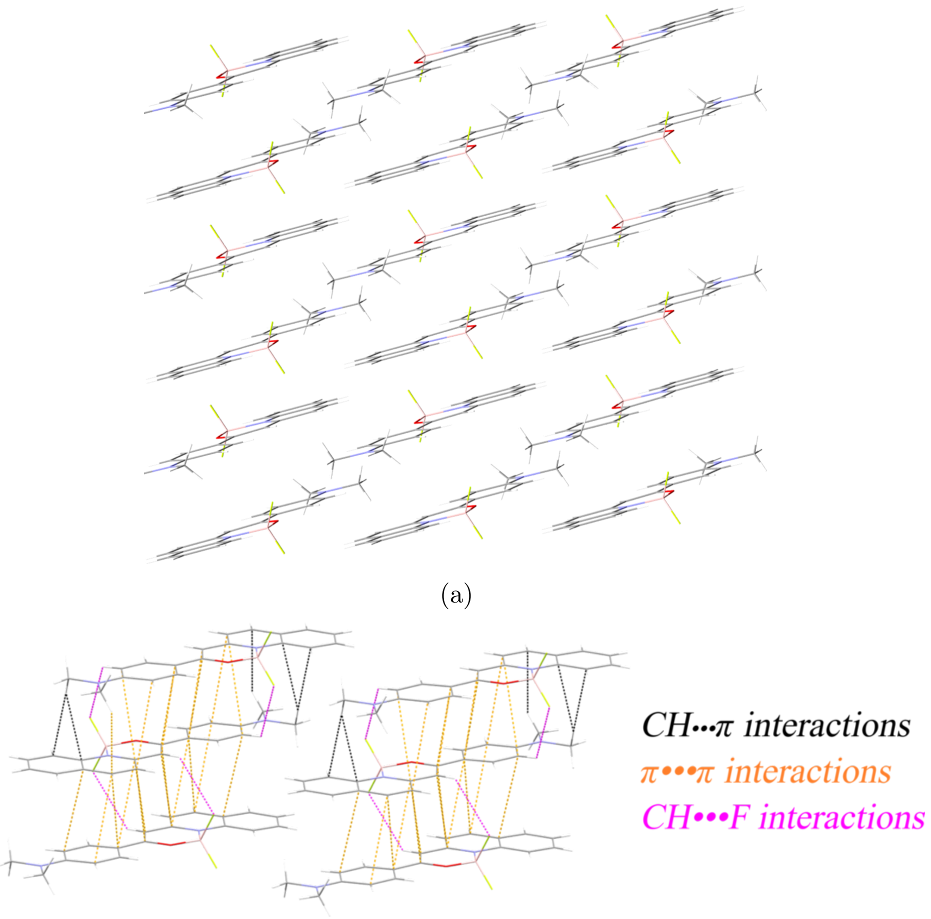

(a)

(b)

Figure S4: Molecular packing of **2**: (a) side view; (b) indication of intermolecular interactions in crystal structure.

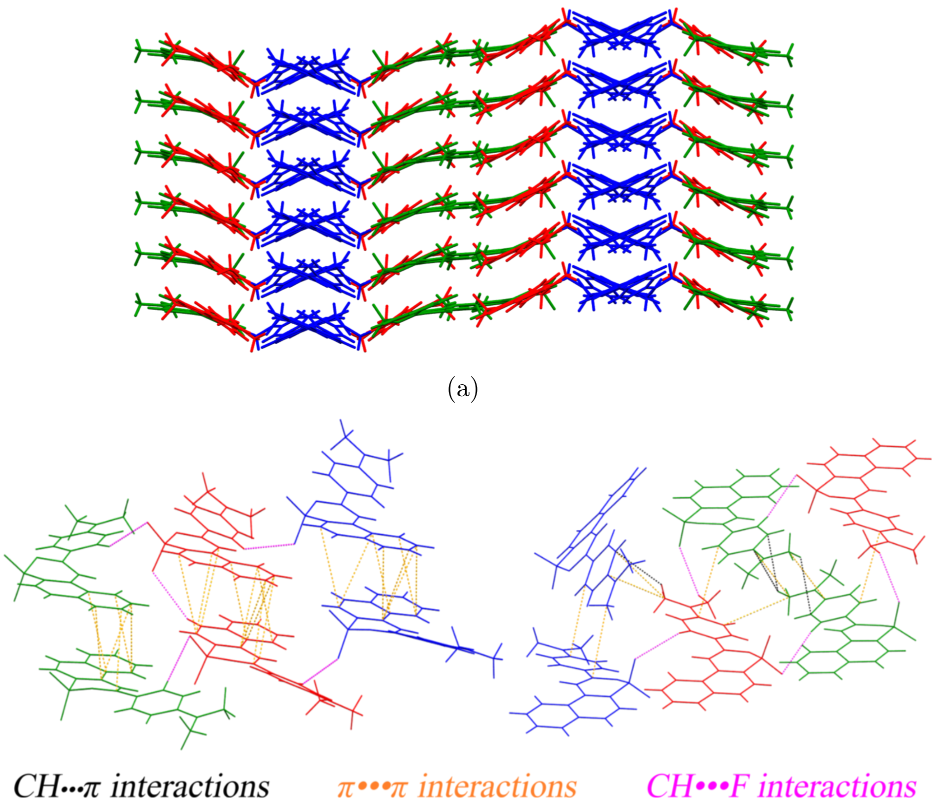

(a)

(b)

Figure S5: Molecular packing of **3**: (a) side view; (b) indication of intermolecular interactions in crystal structure.

$X, \frac{1}{2}+Y, Z]$. The Cg···Cg distance, dihedral angle between these rings, angle between Cg and normal to the second ring, and slippage parameters are 3.715(2) Å, 1.6(2)°, 23.8°, and 1.500 Å, and 3.715(2) Å, 1.6(2)°, 24.6°, and 1.548 Å, respectively, indicating the significant slippage of the interacting B rings. The interaction of B ring with C$[\frac{3}{2}-X, \frac{1}{2}+Y, Z]$ was also found with the parameters described above being 3.526(3) Å, 1.9(2)°, 14.5°, and 0.880 Å, indicating a spatial fit of the two rings better than that of B···B. These interactions might be analyzed as B···(B+C)$[\frac{3}{2}-X, \frac{1}{2}+Y, Z]$, with the respective parameters 3.415(3) Å, 1.7(2)°, 6.0°, and 0.358 Å. The resulting position of the B ring is shifted from the ideal stacking position and is intermediate between the B and C rings of the neighbouring molecule. The observed packing reveals the overlay of (B+C) and (C+E)$[\frac{3}{2}-X, \frac{1}{2}+Y, Z]$, with the parameters of 3.624(2) Å, 1.9(1)°, 19.8°, and 1.230 Å.

Slightly different stacking interactions between the aromatic rings are found for molecules **b**. Ring C forms interactions with C$[\frac{3}{2}-X, -\frac{1}{2}+Y, Z]$ and C$[\frac{3}{2}-X, \frac{1}{2}+Y, Z]$ with the Cg···Cg distance, dihedral angle between rings, angle between Cg and normal to the second ring, and slippage parameters – 3.670(2) Å, 4.7(2)°, 25.4°, and 1.576 Å, and 3.670(2) Å, 4.7(2) °, 23.9°, and 1.485 Å, respectively. The other interaction is found between the C and E $[\frac{3}{2}-X, -\frac{1}{2}+Y, Z]$ rings, the key parameters being 3.530(3) Å, 5.2(2)°, 14.6°, and 0.891 Å. This shows that the origin of interactions is different from that found for molecules **c** and can be summarized as C···(C+E)$[\frac{3}{2}-X, -\frac{1}{2}+Y, Z]$ and (C+E)$[\frac{3}{2}-X, \frac{1}{2}+Y, Z]$, the corresponding parameters being 4.030(2) Å, 3.07(18)°, 35.9°, and 2.366Å, and 4.025(2) Å, 3.07(18)°, 32.1°, and 2.142 Å. Ring moieties (B+C) and (C+E)$[\frac{3}{2}-X, \frac{1}{2}+Y, Z]$ are involved in the interactions with the parameters of 3.559(2) Å, 3.35(14)°, 18.4°, and 1.222 Å.

Molecules **a**, similarly to **b**, are involved in $\pi\cdots\pi$ interaction between C rings – C···C$[\frac{3}{2}-X, -\frac{1}{2}+Y, Z]$ and C···C$[\frac{3}{2}-X, \frac{1}{2}+Y, Z]$. The Cg···Cg distance, dihedral angle between rings, angle between Cg and normal to the second ring, and slippage parameters are 3.644(2) Å, 4.5(2)°, 25.0° and 1.539 Å for first C···C interaction. Similarly, for C···C$[\frac{3}{2}-X, \frac{1}{2}+Y, Z]$ the above mentioned parameters are: 3.644(2) Å, 4.5(2)°, 24.2°, and 1.495 Å. Another interaction type found in the crystal structure is C$\cdots$E$[\frac{3}{2}-X,\frac{1}{2}+Y,Z]$ with parameters of 3.575(3) Å, 3.8(2)°, 18.0°, and 1.107 Å. The C$\cdots$(B+C)$[\frac{3}{2}-X,\frac{1}{2}+Y,Z]$ and C$\cdots$(C+E)$[\frac{3}{2}-X,\frac{1}{2}+Y,Z]$ are determined as well in the packing of molecules **a** with the respective parameters: 3.879(2) Å, 4.2(2)°, 34.1°, and 2.173 Å, and 3.398(2) Å, 4.2(2) °, 9.7°, and 0. 715 Å.

The C–H$\cdots$Cg interactions are found for molecules **c** and involve C18-H18B and the phenyl C12–C17 ring A, with the H$\cdots$Cg$[1-X,2-Y,1-Z]$ distance of 2.86 Å and C–H$\cdots$Cg angle 150°. The intermolecular H-bonds are found between different molecules – C6–H6A$\cdots$F41$[\frac{3}{2}-X,-Y,-\frac{1}{2}+Z]$ and C46–H46A$\cdots$F21, with the respective C$\cdots$F distances and C–H$\cdots$F angles being 3.325(6) Å 145°, and 3.192(6) Å 142° (Table S8).

The molecules of **4** are arranged in a "herring-bone" motif (Figure S6a). In the crystal lattice, the following interactions are found: $\pi\cdots\pi$, C–H$\cdots\pi$, C–H$\cdots$O, and C–H$\cdots$F interactions (Tables S7 and S8, see Figure S6b). The network of the $\pi\cdots\pi$ interactions is formed within crystal structure of **4**. Ring B forms the B$\cdots$E$[-\frac{1}{2}+X,Y,\frac{1}{2}-Z]$ and B$\cdots$E$[\frac{1}{2}+X,Y,\frac{1}{2}-Z]$ interactions with the Cg$\cdots$Cg distance, dihedral angle between rings, angle between Cg and normal to the second ring, and slippage parameters – 3.884(2) Å, 5.2(1)°, 24.8° and 1.626 Å, and 4.008(2) Å, 5.2(1)°, 26.3°, and 1.777 Å, respectively. There is C$\cdots$C$[-\frac{1}{2}+X,Y,\frac{1}{2}-Z]$ interactions with parameters 3.874(2) Å, 4.3(1)°, 23.0°, and 1.515 Å. C rings are involved in C$\cdots$D$[-\frac{1}{2}+X,Y,\frac{1}{2}-Z]$ and C$\cdots$E$[\frac{1}{2}+X,Y,\frac{1}{2}-Z]$ interactions with above mentioned parameters – 3.856(2) Å, 5.3(1)°, 24.3°, and 1.584 Å, and 3.685(2) Å, 2.5(1)°, 15.0°, and 0.795 Å. The interactions between D rings are also found in the structure – D$\cdots$D$[-\frac{1}{2}+X,Y,\frac{1}{2}-Z]$ and D$\cdots$D$[\frac{1}{2}+X,Y,\frac{1}{2}-Z]$ with parameters – 3.811(2) Å, 5.9(1)°, 21.8° and 1.412 Å, and 3.811(2) Å, 5.9(1)°, 25.3°, and 1.627 Å. The C22–H22B$\cdots\pi$ interactions are formed by methyl group of the aniline moiety and aniline ring A$[-\frac{1}{2}+X,-\frac{1}{2}-Y,-Z]$ with the H$\cdots$Cg distance of 2.94 Å and angle between H–Cg and the line perpendicular to the A$[-\frac{1}{2}+X,-\frac{1}{2}-Y,-Z]$ ring being 10.65°.

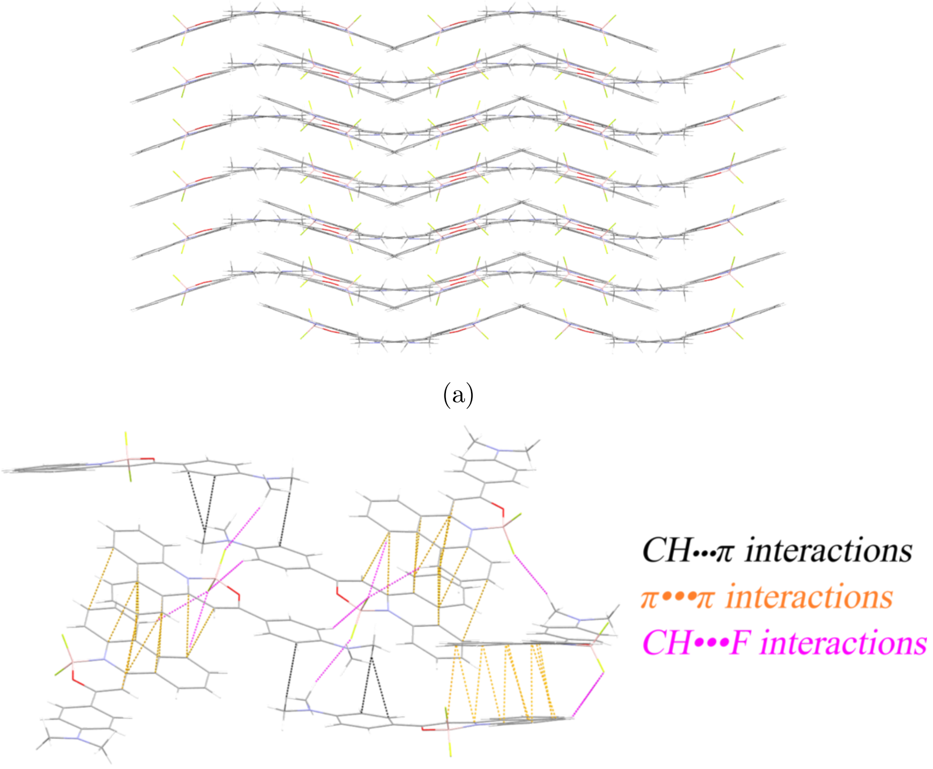

(a)

(b)

Figure S6: Molecular packing of **4**: (a) side view; (b) indication of intermolecular interactions in crystal structure.

Table S6: Crystal data and structure refinement parameters for **2**-**4**.

Compound	**2**	**3**	**4**
Empirical formula	$C_{19}H_{17}BF_2N_2O$	$C_{19}H_{17}BF_2N_2O$	$C_{23}H_{19}BF_2N_2O$
Formula weight	338.15	338.15	388.21
Shape / color	block / red	needle / orange	needle / red
Crystal size [mm]	0.70 × 0.36 × 0.21	0.52 × 0.14 × 0.05	0.53 × 0.14 × 0.10
Crystal system	Triclinic	Orthorhombic	Orthorhombic
Space group	P-1	Pbca	Pbca
a[Å]	7.9326(10)	30.6090(18)	7.4012(9)
b[Å]	8.4946(9)	7.2702(5)	18.135(2)
c[Å]	12.4339(14)	44.556(2)	27.312(3)
α[°]	83.493(9)	90	90
β[°]	75.117(10)	90	90
γ[°]	84.165(10)	90	90
Volume [Å^3]	802.22(17)	9915.3(10)	3665.7(7)
Z	2	24	8
Density (calc.) [g/cm^3]	1.400	1.359	1.407
Absorption coefficient [mm^{-1}]	0.102	0.099	0.100
F(000)	352	4224	1616
Θ range [°]	2.420 to 28.227	2.195 to 23.999	2.367 to 28.626
Reflections collected / unique	5246 / 3516 [R(int) = 0.0386]	52584 / 7780 [R(int) = 0.1731]	11559 / 4213 [R(int) = 0.0866]
Index ranges hkl	$-9 \leq h \leq 10$, $-11 \leq k \leq 8$, $-14 \leq l \leq 16$	$-34 \leq h \leq 35$, $-8 \leq k \leq 8$, $-50 \leq l \leq 49$	$-9 \leq h \leq 7$, $-24 \leq k \leq 10$, $-29 \leq l \leq 35$
Restraints/parameters	0 / 227	0 / 676	0 / 262
Max. and min. transmission	0.980 and 0.947	0.996 and 0.969	0.991 and 0.976
Goodness of fit on F^2	1.022	1.037	0.966
Final R indices [$I > 2\sigma(I)$]	R1 = 0.0551, wR2 = 0.1263	R1 = 0.0890, wR2 = 0.1684	R1 = 0.0632, wR2 = 0.1327
R indices (all data)	R1 = 0.0886, wR2 = 0.1533	R1 = 0.1835, wR2 = 0.2093	R1 = 0.1564, wR2 = 0.1783
Largest diff. peak and hole eÅ^{-3}	0.169 and −0.227	0.250 and −0.233	0.224 and −0.242

Table S7: Selected parameters [Å, °] for **1-4**.

	1	**2**	**3**	**4**
Dihedral angle NMe$_2$–Phe	4.0 12.9	3.3	3.2 – 4.3	7.3
Dihedral angle Phe–Ar	4.2 – 4.7	2.5	15.1 – 18.0	13.4
RMSD B$\cdots$N–C3–O	0.330 – 0.364	0.047	0.258 – 0.357	0.007
B–N1	1.579 – 1.583	1.598(2)	1.562(6) – 1.573(6)	1.583(4)
B–O1	1.434 – 1.436	1.457(3)	1.435(6) – 1.456(6)	1.445(4)
O1–C	1.340 – 1.345	1.332(2)	1.326(5) – 1.339(5)	1.320(3)
N1–C	1.361 – 1.363	1.357(2)	1.343(5) – 1.360(5)	1.347(3)
$\pi\cdots\pi$	3.76	3.71-3.95	3.39-3.97	3.59-3.89
CH$\cdots\pi$	2.68-2.98	2.98	2.86	2.94
CH$\cdots$F	2.54-2.80	2.38-2.56	2.40-2.81	2.62-2.80

Table S8: C–H$\cdots$F and C–H$\cdots$O interactions [Å, °] for **2-4**.

D–H$\cdots$A	**d(D–H)**	**d(H$\cdots$A)**	**<DHA)**	**d(D$\cdots$A)**
		2		
C2–H2A$\cdots$F1	0.93	2.38	119	2.943(2)
C2–H2A$\cdots$F2	0.93	2.56	115	3.068(2)
C17–H17A$\cdots$O1	0.93	2.42	101	2.756(2)
		3		
C6–H6A$\cdots$F4[a]	0.93	2.52	145	3.325(6)
C46–H46A$\cdots$F21	0.93	2.40	142	3.192(6)
C37–H37A$\cdots$O21	0.93	2.40	100	2.727(6)
C57–H57A$\cdots$O41	0.93	2.40	101	2.733(6)
		4		
C2–H2A$\cdots$F1	0.93	2.46	114	2.966(4)
C2–H2A$\cdots$F2	0.93	2.30	121	2.888(3)
C17–H17A$\cdots$O1	0.93	2.44	100	2.748(4)

[a] Symmetry code: $\frac{3}{2} - X, -Y, -\frac{1}{2} + Z$

Calculations of intermolecular interaction energies

The total intermolecular interaction energy was calculated for a subset of dimers obtained for **1**-**4** (Table S10) at both ωB97X-D/*aug*-cc-pVTZ and ωB97X-D/*aug*-cc-pVDZ levels of theory using Gaussian 16.[2] The total intermolecular energies were calculated using the supermolecular approach without ($\Delta E_{\mathrm{int}}^{\mathrm{total,noCP}}$) and with counterpoise (CP) correction ($\Delta E_{\mathrm{int}}^{\mathrm{total,CP}}$).[3] The basis set superposition error (BSSE)[4] can be calculated as difference between these two energies:

$$\mathrm{BSSE} = \Delta E_{\mathrm{int}}^{\mathrm{total,noCP}} - \Delta E_{\mathrm{int}}^{\mathrm{total,CP}} \tag{2}$$

The results of these calculations are given in Table S9.

Table S9: Results of total intermolecular interaction energy calculations using ωB97X-D/*aug*-cc-pVTZ and ωB97X-D/*aug*-cc-pVDZ levels of theory for selected dimers of **1**-**4**. [a]

Dimer	***aug*-cc-pVTZ**			***aug*-cc-pVDZ**		
	$\boldsymbol{\Delta E_{\mathrm{int}}^{\mathrm{total,noCP}}}$	$\boldsymbol{\Delta E_{\mathrm{int}}^{\mathrm{total,CP}}}$	**BSSE**	$\boldsymbol{\Delta E_{\mathrm{int}}^{\mathrm{total,noCP}}}$	$\boldsymbol{\Delta E_{\mathrm{int}}^{\mathrm{total,CP}}}$	**BSSE**
$1\mathrm{ba}_{\pi\pi}$	-11.19	-10.75	-0.44	-13.09	-11.07	-2.02
$1\mathrm{ab}_{\mathrm{T}\pi}$-1	-11.94	-11.24	-0.7	-15.41	-11.66	-3.75
$2\mathrm{aa}_{\pi\pi}$-1	-25.34	-24.21	-1.13	-31.1	-25	-6.1
$2\mathrm{aa}_{\pi\pi}$-2	-26.62	-25.48	-1.14	-31.93	-26.26	-5.67
$3\mathrm{aa}_{\pi\pi}$	-18.48	-17.62	-0.86	-22.26	-18.21	-4.05
$3\mathrm{bb}_{\pi\pi}$	-17.52	-16.71	-0.81	-20.95	-17.3	-3.65
$3\mathrm{cc}_{\pi\pi}$	-17.54	-16.79	-0.75	-21.33	-17.39	-3.94
$4\mathrm{aa}_{\pi\pi}$	-23.13	-22.16	-0.97	-27.72	-22.87	-4.85

[a] All values are given in kcal/mol.

Table S10: Structures of dimers chosen for intermolecular interaction energy decomposition calculations for **1-4** and **4(H)**.

Comp	Structure of dimer complexes studied herein		
1	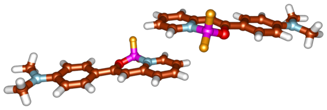 **1ba**$_{\pi\pi}$	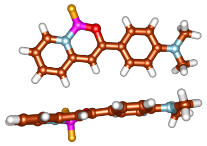 **1ab**$_{\mathrm{T}\pi}$**-1**	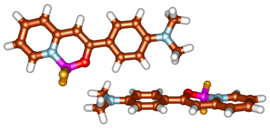 **1ab**$_{\mathrm{T}\pi}$**-2**
2	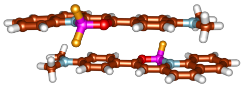 **2aa**$_{\pi\pi}$**-1**	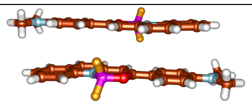 **2aa**$_{\pi\pi}$**-2**	
3	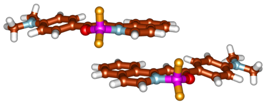 **3aa**$_{\pi\pi}$	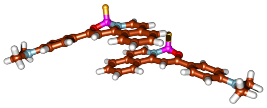 **3bb**$_{\pi\pi}$	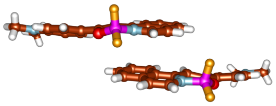 **3cc**$_{\pi\pi}$
	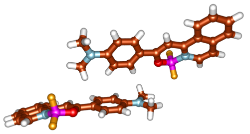 **3bb**$_{\mathrm{T}\pi}$	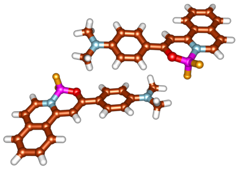 **3ca**$_{\mathrm{T}\pi}$	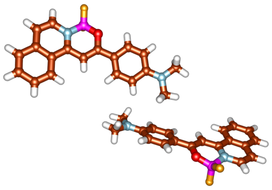 **3ba**$_{\mathrm{CH}\pi}$
	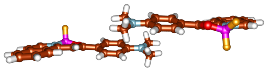 **3cc**$_{\mathrm{CH}\pi}$		
4	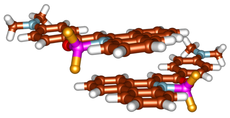 **4aa**$_{\pi\pi}$	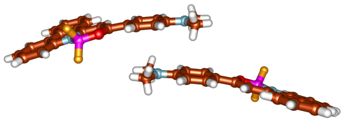 **4aa**$_{\mathrm{CH}\pi}$	
4(H)	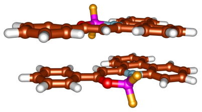 **4(H)**$_{\pi\pi}$		

Cartesian coordinates for optimized structures

Compound 1

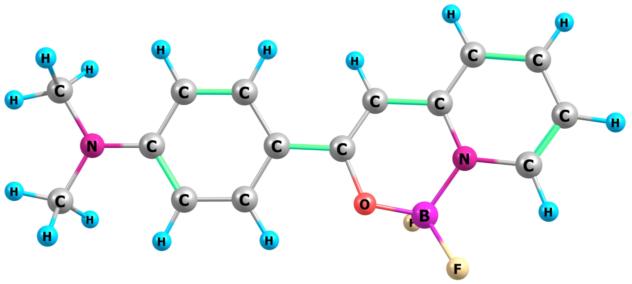

C	-4.570851	-0.353776	-0.243035
N	-3.195429	-0.204251	-0.097016
C	-2.696366	1.059291	0.079430
C	-3.492393	2.168603	0.133057
C	-4.934189	2.025820	0.022112
C	-5.422688	0.744437	-0.172334
C	-1.221582	1.129152	0.148452
C	-0.432390	0.042502	-0.086617
O	-0.907318	-1.171645	-0.317158
C	1.045250	0.120250	-0.068553
C	1.765406	1.335758	-0.085546
C	3.144355	1.359184	-0.062257
C	3.891767	0.147382	-0.027081
C	3.167041	-1.077964	-0.023490
C	1.787600	-1.080930	-0.045795
N	5.261622	0.160549	-0.001241
C	6.014940	-1.089790	0.029610
C	5.991743	1.424150	-0.003655
B	-2.318819	-1.496701	0.067577
F	-2.787956	-2.474207	-0.785037
F	-2.331298	-1.910167	1.392093
H	-4.909817	-1.364781	-0.409706
H	-6.489950	0.567893	-0.276178
H	-5.588042	2.885042	0.095589
H	-3.034680	3.144627	0.245302
H	-0.783343	2.094493	0.363476
H	1.233789	2.278572	-0.135117
H	3.651932	2.314735	-0.081295
H	3.692237	-2.024049	-0.001350
H	1.238881	-2.014414	-0.044208
H	7.079967	-0.865124	0.044549
H	5.772905	-1.675766	0.923163
H	5.803333	-1.701189	-0.854530
H	7.060498	1.220173	0.029768
H	5.779302	2.003146	-0.909529
H	5.729699	2.034176	0.867959

Compound 2

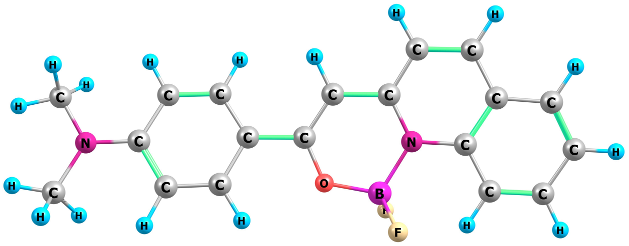

C	-3.651110	-0.048812	0.005225
N	-2.249814	0.027251	0.019641
C	-1.645474	1.255132	-0.058297
C	-2.362914	2.431884	-0.147082
C	-3.774890	2.399545	-0.169967
C	-4.432431	1.162550	-0.095020
C	-0.179165	1.275785	-0.040810
C	0.567741	0.146927	0.055677
O	0.045966	-1.064828	0.130529
C	2.053206	0.156486	0.041804
C	2.822763	1.317643	0.262683
C	4.203519	1.285537	0.233839
C	4.896216	0.067319	-0.012727
C	4.119982	-1.106053	-0.220475
C	2.739682	-1.053396	-0.189968
N	6.268698	0.025440	-0.043774
C	6.965546	-1.233126	-0.286303
C	7.052153	1.236318	0.172017
B	-1.415621	-1.333484	0.097190
F	-1.688047	-2.091487	-1.028265
F	-1.746460	-2.001013	1.263495
C	-4.312478	-1.287417	0.083912
C	-5.852183	1.048310	-0.113712
H	-4.352779	3.314052	-0.247596
H	-1.823247	3.370115	-0.202225
H	0.292722	2.245212	-0.128506
H	2.330524	2.258840	0.478341
H	4.751917	2.201080	0.413582
H	4.603063	-2.056943	-0.404779
H	2.153014	-1.950851	-0.342551
H	8.039637	-1.056577	-0.270296
H	6.725318	-1.973963	0.484779
H	6.698551	-1.651704	-1.263316
H	8.111182	0.996961	0.092987
H	6.814339	2.000169	-0.577025
H	6.866696	1.657538	1.166993
C	-5.703991	-1.354363	0.062339
C	-6.472944	-0.183625	-0.037036
H	-3.736707	-2.196590	0.165125
H	-6.436848	1.960806	-0.190439
H	-6.190218	-2.322734	0.123506
H	-7.557791	-0.245558	-0.053491

Compound 3

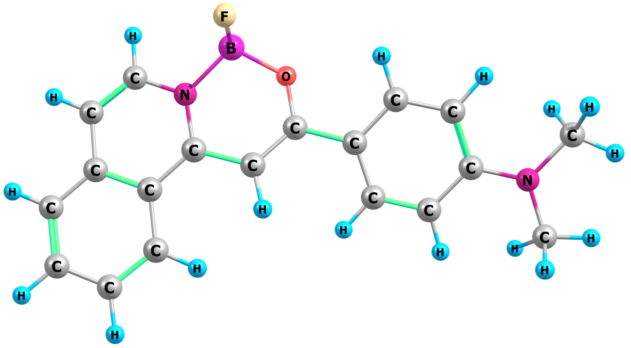

C	4.004561	-3.268205	-0.216985
C	3.586282	1.737299	0.280190
N	2.312512	1.300684	0.106996
C	2.067399	-0.046847	-0.048656
C	3.117124	-0.989491	-0.057173
C	4.476811	-0.519566	0.102941
C	4.658700	0.886865	0.284425
C	0.656377	-0.407768	-0.123138
C	-0.339473	0.494768	0.117833
O	-0.114957	1.785582	0.357220
C	-1.776594	0.126937	0.099180
C	-2.236840	-1.200947	0.222280
C	-3.584608	-1.505778	0.187247
C	-4.557214	-0.479020	0.038078
C	-4.094716	0.861194	-0.065975
C	-2.742358	1.146099	-0.035094
N	-5.900691	-0.772704	0.003030
C	-6.885924	0.291036	-0.148491
C	-6.359804	-2.150935	0.118061
B	1.164199	2.381247	-0.094249
F	1.086735	2.698565	-1.440688
F	1.458165	3.478234	0.687782
C	5.543911	-1.426862	0.091873
C	2.921030	-2.402028	-0.209160
H	0.399897	-1.430320	-0.354456
H	-1.525657	-2.006267	0.366759
H	-3.889658	-2.539326	0.288477
H	-4.798515	1.676985	-0.170722
H	-2.395715	2.169308	-0.112928
H	-7.884194	-0.143501	-0.157257
H	-6.828140	1.007244	0.679664
H	-6.738827	0.837668	-1.087296
H	-7.446827	-2.173135	0.060660
H	-5.958931	-2.772017	-0.691688
H	-6.055768	-2.593229	1.074312
C	5.318264	-2.800807	-0.070551
H	6.553589	-1.046105	0.218590
H	6.151231	-3.496076	-0.078533

H	3.826779	-4.333819	-0.338632
H	1.921909	-2.805423	-0.320827
H	3.686187	2.807191	0.412675
H	5.656870	1.287214	0.429348

Compound 4

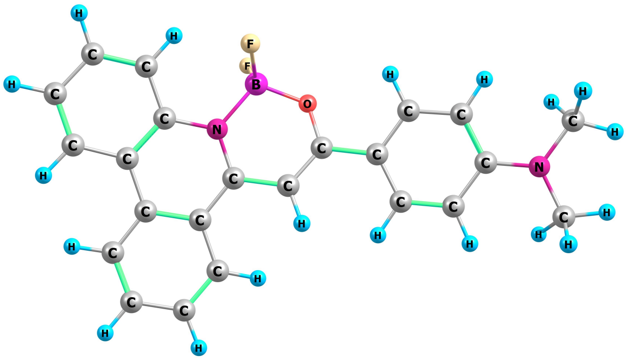

C	-2.646827	4.069258	0.085149
C	-3.116989	-1.014317	-0.056679
N	-1.757633	-0.741710	0.049123
C	-1.319664	0.560641	0.015275
C	-2.207087	1.658526	0.017780
C	-3.627952	1.426870	-0.025518
C	-4.079385	0.041511	-0.099991
C	0.124650	0.751407	-0.046672
C	1.012724	-0.256837	0.184750
O	0.630019	-1.488906	0.483033
C	2.481527	-0.081696	0.103952
C	3.112624	1.180054	0.100552
C	4.486812	1.301577	0.019261
C	5.315131	0.147781	-0.054666
C	4.680433	-1.123809	-0.037154
C	3.304038	-1.225946	0.040329
N	6.683312	0.259478	-0.137089
C	7.517951	-0.932927	-0.217085
C	7.319146	1.570551	-0.144929
B	-0.741664	-1.971741	0.219595
F	-0.742033	-2.713571	-0.953748
F	-1.134136	-2.726909	1.307944
C	-3.564120	-2.358278	-0.143563
C	-5.440674	-0.301909	-0.216135
C	-4.500548	2.520068	-0.009719
C	-1.752985	3.019614	0.076291
H	0.492942	1.723620	-0.334454
H	2.517173	2.082482	0.179868
H	4.924808	2.291359	0.021429
H	5.269600	-2.030713	-0.084050
H	2.827401	-2.198498	0.055833

H	8.563251	-0.635104	-0.282298
H	7.394250	-1.565863	0.669738
H	7.273576	-1.530555	-1.103144
H	8.398428	1.445476	-0.216240
H	6.984818	2.170279	-0.999955
H	7.096940	2.126743	0.773657
C	-4.910424	-2.650178	-0.251162
C	-5.861027	-1.620216	-0.286115
H	-2.841779	-3.159322	-0.136384
H	-6.183619	0.485609	-0.259169
H	-5.225863	-3.687250	-0.316473
H	-6.918769	-1.849170	-0.374988
C	-4.032136	3.835019	0.040249
H	-5.571470	2.353796	-0.031068
H	-4.732327	4.663516	0.051120
H	-2.272428	5.088305	0.137143
H	-0.694301	3.234578	0.150000

HOMO – LUMO orbitals

Table S11: Kohn-Sham frontier orbitals of **1-4** calculated at the XMC-QDPT2(10,10)/6-31G(d,p) level of theory.

Compound	HOMO	LUMO
1	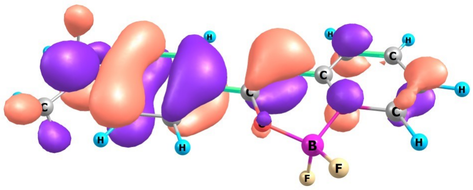	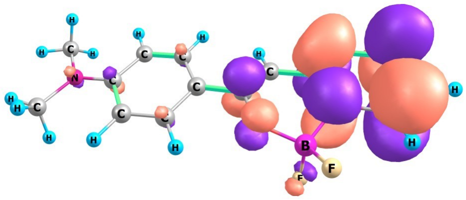
2	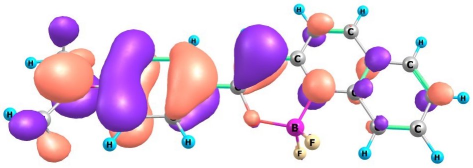	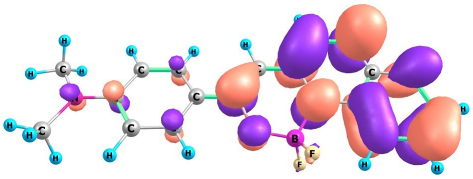
3	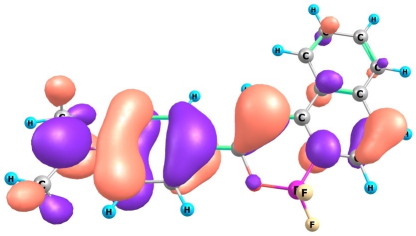	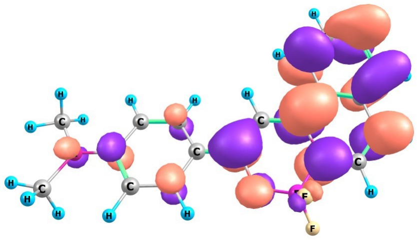
4	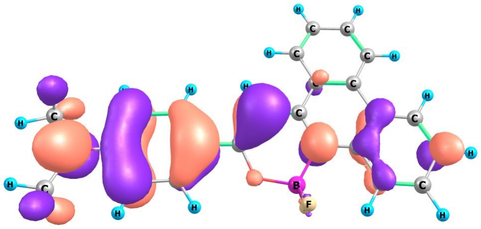	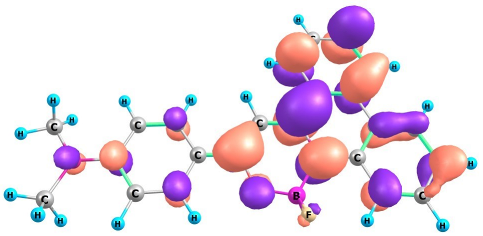

References

(1) Spek, A. L. Single-Crystal Structure Validation with the Program *PLATON*. *J. Appl. Crystallogr.* **2003**, *36*, 7–13.

(2) Frisch, M. J. et al. Gaussian~16 Revision C.01. 2019; Gaussian Inc. Wallingford CT.

(3) Boys, S. F.; Bernardi, F. The Calculation of Small Molecular Interactions by the Differences of Separate Total Energies. Some Procedures with Reduced Errors. *Mol. Phys.* **1970**, *19*, 553–566.

(4) van Duijneveldt, F. B.; van Duijneveldt-van de Rijdt, J. G. C. M.; van Lenthe, J. H. State of the Art in Counterpoise Theory. *Chem. Rev.* **1994**, *94*, 1873–1885.